New 40 Ar/ 39 Ar constraints for the "Grande Nappe": The largest rhyolitic eruption from the Mont-Dore Massif (French Massif Central)

Sébastien Nomade, Jean-François Pastre, Alison Pereira, Alexandra Courtin-Nomade, Vincent Scao

Petrology, Geochemistry (Geochronology)

New ^{40}Ar/^{39}Ar constraints for the "Grande Nappe": The largest rhyolitic eruption from the Mont-Dore Massif (French Massif Central)

Sébastien Nomade [a,*], Jean-François Pastre [b], Alison Pereira [a,c,d,e], Alexandra Courtin-Nomade [f], Vincent Scao [a]

[a] *Laboratoire des sciences du climat et de l'environnement (IPSL-CEA-CNRS-UVSQ) et Université Paris-Saclay, domaine du CNRS, bât. 12, avenue de la Terrasse, 91198 Gif-sur-Yvette, France*
[b] *Laboratoire de géographie physique, Environnements quaternaires et actuels, UMR 8591 CNRS, Universités Paris-1 et Paris-12, 1, place Aristide-Briand, 92195 Meudon cedex, France*
[c] *Département de préhistoire du Muséum national d'histoire naturelle, UMR 7194 du CNRS, 1, rue René-Panhard, 75013 Paris, France*
[d] *Sezione di science preistoriche e antropologiche, Dipartimento di Studi Umanistici, Università degli Studi di Ferrara, C.so Ercole d'Este I, 32 Ferrara, Italy*
[e] *École française de Rome, Piazza Farnese, 00186 Roma, Italy*
[f] *Université de Limoges, GRESE, EA 4330, FST, 123, avenue Albert-Thomas, 87060 Limoges, France*

A B S T R A C T

Since the 1960s, an early explosive activity in the Mont-Dore Massif is associated with a major pyroclastic rhyolitic eruption (5–7 km^3) known as the "Grande Nappe" (GN). This event, linked to the formation of a 6-km-diameter cryptic caldera named "Haute Dordogne", was before our investigation dated by ^{40}Ar/^{39}Ar at 3.07 ± 0.04 Ma. Our new single-crystal laser fusion ^{40}Ar/^{39}Ar dates obtained on two outcrops of the GN (Rochefort-Montagne and Ludières) questioned several hypotheses made concerning this "landmark" event of the Mont-Dore Massif history. We demonstrate that: (1) the GN rhyolitic eruption has occurred much later than previously estimated (*i.e.* 2.77 ± 0.02–0.07 Ma full external uncertainties); (2) the correlation made between the Vendeix rhyolitic complexes (intra-caldera position) dated back to 2.74 ± 0.04 Ma and the GN is proposed; (3) xenocryst contamination could be very high (*i.e.* 70% for the Rochefort-Montagne GN outcrop) and explains the noticeable older age obtained previously; (4) a link between the GN eruption and the formation of a caldera is questionable; the hypothesis of a northward-oriented blast channeled eastward toward the paleo-Allier River is thus proposed.

© 2017 Académie des sciences. Published by Elsevier Masson SAS. This is an open access article under the CC BY-NC-ND license (http://creativecommons.org/licenses/by-nc-nd/4.0/).

1. Introduction

Two large stratovolcanoes are known in the French Massif Central: the Cantal and the Mont-Dore Massif (Fig. 1). The youngest of these edifices (Mont-Dore) covers an area of 500 km^2 and rests on the Variscan basement (Cantagrel and Baubron, 1983). The total volume erupted from the Mont-Dore Massif has been estimated between 220 km^3 and 70 km^3 (Brousse, 1971; Cantagrel and Baubron, 1983; Cantagrel and Briot, 1990; Vincent, 1980; Fig. 1). This massif is composed of two coalescent stratovolcanoes: the Guéry and the Sancy (Cantagrel and Baubron, 1983; Nomade et al., 2014a; Pastre and Cantagrel, 2001). The diversity and the wide dispersion of its
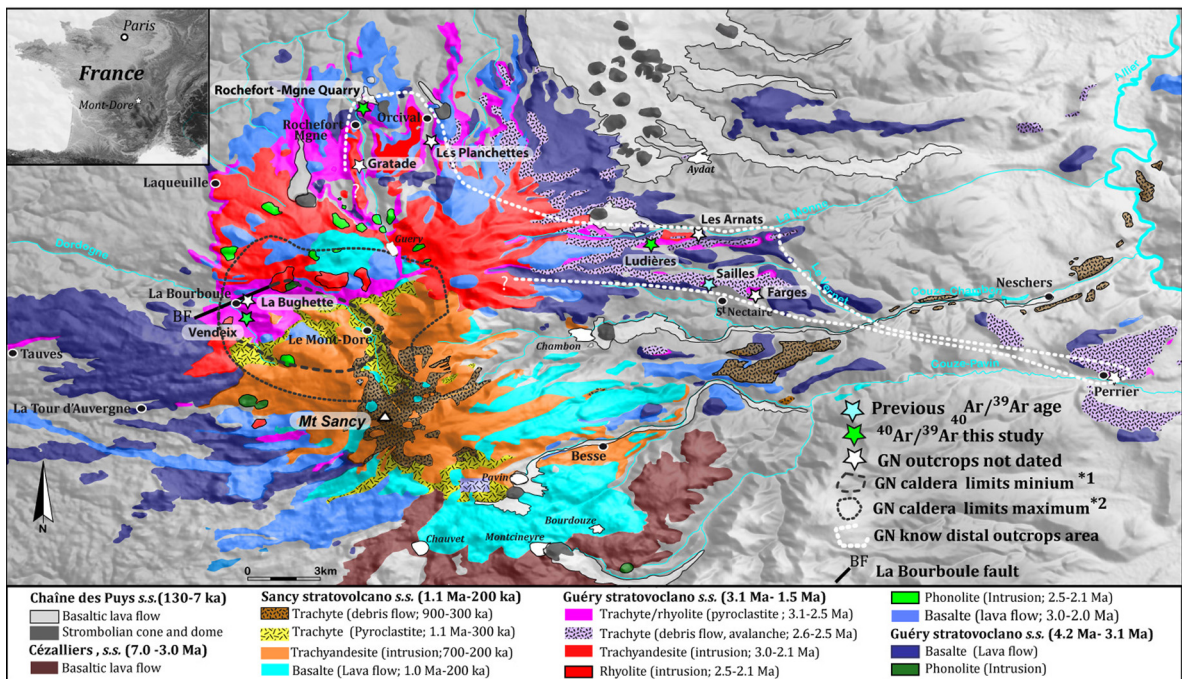
Fig. 1. Mont-Dore Massif synthetic geological map and sampling location (modified from Cantagrel and Baubron, 1983). The Mont-Dore Massif is constituted by the Sancy and Guéry stratovolcanoes (Pastre and Cantagrel, 2001). The lower and upper extension limits of the GN caldera are from Mossand et al. (1982) and Varet et al. (1980), respectively.

pyroclastic products have been used for stratigraphic correlation and dating of the Plio-Pleistocene formations in the French Massif Central and elsewhere (Degeai et al., 2013; Nomade et al., 2010; Pastre and Cantagrel, 2001; Pastre et al., 2015). Several recent ^{40}Ar/^{39}Ar investigations have allowed refining the history of the Mont-Dore Massif explosive activity (Nomade et al., 2012, 2014a,b). These new chronological constraints have highlighted that the pyroclastic activity of the massif was more complex that previously thought and comprised of eight cycles (3.1 Ma to 300 ka) lasting about 100 ka each (Nomade et al., 2014a). Despite these recent efforts, several questions remain open, in particular among the early explosive activity of the Guéry stratovolcano (cycle G.I and G.II in Nomade et al., 2014a). The accurate age, the volume and the origin of the iconic rhyolitic eruption known as the "Grande Nappe" (GN hereafter; Vincent, 1979; 1980) remain elusive, mainly because of the lack of single crystal ^{40}Ar/^{39}Ar investigation.

2. The "Grande Nappe": geological background and current age constraints

The term "Grande Nappe", created by Vincent (1979, 1980), designates the main pyroclastic formation of Mont-Dore with a rhyolitic composition. This "eruption" is also known under different names: "nappe supérieure" (Brousse, 1963), "nappe rhyolitique", "nappe de Rochefort" and "nappe of Sailles" (Besson, 1978), "nappe externe" (Brousse, 1984), or Mont-Dore ignimbrite (Pastre and Cantagrel, 2001). According to the original suggestion

of Vincent (1979), the GN includes under this general name all rhyolitic products found under "the intermediate complex" defined by this author and the "upper pumice stones" found in the external flanks of the Mont-Dore. The formation of this GN is suggested to be linked to the formation of a cryptic caldera named C1 or "Haute-Dordogne" (Vincent, 1979, 1980). The limit of this caldera remains unclear as traces of this depression are probably buried below more recent products. From a chronological point of view, we now know that in the internal part of the Guéry stratovolcano the "upper pumice stones" correspond in reality to several trachytic pyroclastic units emplaced in two phases (G.II: 2.73–2.60 Ma and G.III: 2.40–1.95 Ma) as well as to the younger Sancy stratovolcano starting to erupt much later, at about 1.1 Ma (C.I.) (Nomade et al., 2012, 2014a). Therefore, the GN is by definition older than 2.73 ± 0.02 Ma, which is the age of the oldest trachytic pyroclastic rock located above the GN (La Bourboule Haut, Nomade et al., 2014a). The current age of the GN (i.e. 3.07 ± 0.04 Ma (2σ uncertainty), Féraud et al., 1990; Fig. 1) corresponds to the weighted mean of three independent ages (i.e. sanidine populations including 5–7 crystals) coming from a single outcrop (i.e. Sailles). Because of the ubiquist xenocrystic contamination of the Guéry pyroclastic products shown in Nomade et al. (2014a), the accuracy of this age could legitimately be questioned.

Historically, the GN outcrops were divided into two groups: proximal/internal or distal/external deposits corresponding to outcrops found inside (e.g., Brousse, 1963; Brousse and Lefèvre, 1966; Ménard, 1979; Pastre, 1987; Pastre and Cantagrel, 2001; Vincent, 1979, 1980)

and outside (Besson, 1978; Ménard et al., 1980; Ly, 1982; Pastre, 1987; Pastre and Cantagrel, 2001) of the limit of what is considered to be the Haute Dordogne caldera limits. The GN volume was estimated between 7 km³ (Brousse and Lefèvre, 1966) and 5 km³ (Vincent, 1980), making it the largest eruptive formation of the Mont-Dore Massif (Equiv. $5 < VEI < 6$; Newhall and Self, 1982). However, the GN eruption remains small compared to the major on-land ignimbrites, which can range between 100 and 3000 km³ (Cas and Wright, 1988).

In the internal zone (*i.e.* intra-caldera), the GN includes the zeolithized facies found in la "Bugette" and the rhyolitic pyroclastite pumiceous flow of Fenestre–Bourboule ("nappe inférieure" of Brousse (1963), Brousse and Lefèvre (1966), Ménard (1979) (Fig. 1) as well as according to Pastre (1987) and Pastre and Cantagrel (2001) all pumiceous surges and flows visible between 1000 and 1040 m a.s.l. in the Vendeix small valley along road D.88 ("intermediate complex" of Vincent, 1979). These pyroclastic rocks are also found throughout the periphery of the La Bourboule city and exposed along the Eau salée ravine and the Vendeix stream (*i.e.* the Vendeix-Siège formation in Nomade et al., 2014a). Between La Bourboule and the southern part of the Vendeix valley, these formations were dropped by 120 m due to the activity of a normal fault visible north of the city of La Bourboule (Fig. 1). In the inner zone, the GN lies on top of the volcano-sedimentary sequence made of tuffites, which followed the trachytic pyroclastic flow of La Bourboule (Pastre, 1987; Pastre and Cantagrel, 2001) or "infrabasale" for Ménard (1979). However, the presence of the GN inside the Bourboule depression, interpreted as the northern edge of the Haute Dordogne caldera, was questioned by the ⁴⁰Ar/³⁹Ar ages obtained by Nomade et al., 2014a (see below), which suggest an age of 2.74 ± 0.02 Ma for the "Vendeix-Siège" formation, which is much younger than the suggested age for the GN (*c.a.* 3.07 ± 0.04 Ma; Féraud et al., 1990).

In the external zone (*i.e.* extra-caldera), the GN outcrops in the northern and eastern borders of the Mont-Dore Massif (Fig. 1), where it has the characteristic facies of a coherent rhyolitic tuff included various amounts of fibrous pumice stones (12–15 m thick in the Rochefort-Montagne old quarry, for example) (Fig. 2) as well as lithic fragments from older volcanic events and Hercynian basements rocks (Féraud et al., 1990). The fibrous pumice stones have an alkaline rhyolite composition (SiO_2 = 73–74% and 33–36% of normative quartz) similar to that of the rhyolite of Lusclade found in the Cantal stratovolcano (Besson, 1978). They represent the ultimate product of the differentiation process by fractional crystallization (Ménard et al., 1980; Villemant et al., 1980). The paragenesis of these subaphyric pumice stones includes alkali feldspars (sanidine), green amphibole (edenite) and magnetite. Quartz, brown amphibole, biotite and titanite are only found in the matrix. Quartz and sanidine crystals are present in the matrix with scarce pyroxene, biotite and titanite (Pastre and Cantagrel, 2001). The GN is suggested to reach the Allier River on the east (Fig. 1) (Ly, 1982; Pastre, 1987). Between the Perrier plateau and Rochefort-Montagne, several outcrops are reported north of Saint-Nectaire – *i.e.* Ludières; Sailles

(3.07 ± 0.04 Ma; Féraud et al., 1990); Farges and Les Arnats (Fig. 1). The eastern extension of the GN was interpreted as the channeling of this eruption in a north- and east–west-oriented system of paleo-valleys (Pastre and Cantagrel, 2001). The same eastward channeling process was proposed for the four debris avalanches due to westward collapses of the Guéry stratovolcano dated back to between 2.61 and 2.58 Ma (Nomade et al., 2014a). These events fossilized the paleo-Allier river and are now exposed in the Perrier plateau sequence (Bernard et al., 2009; Nomade et al., 2014b; Pastre, 2004).

The current volume and the extent of the GN are based on the assumption that virtually all rhyolitic products found north and east of the Mont-Dore belong to this event. As a matter of fact, the "Vendeix-Siege" rhyolitic surges and flows found in the left bank of Vendeix stream in intra-caldera position, considered as an internal equivalent of the GN (Pastre, 1987; Pastre and Cantagrel, 2001), were dated at 2.74 ± 0.02 Ma by Nomade et al. (2014a) (Fig. 1) suggesting that despite their chemical, lithological and mineralogical similarities these two events cannot be correlated anymore. Finally, Nomade et al. (2014b) also dated a rhyolitic pumice fall stratigraphically below the GN in the Perrier Plateau (*i.e.* PER 128 at 3.09 ± 0.01 Ma), suggesting that at least one older event pre-dates the proposed caldera formation and GN eruption (Fig. 1).

In order to start unravel some of the questions raised by the recent geochronological investigations and to improve the precision and accuracy of the GN eruption, we decided to conduct a detailed ⁴⁰Ar/³⁹Ar investigation using single sanidine crystal laser dating on two well-known outcrops both located north and east of the Mont-Dore Massif (*i.e.* Rochefort-Montagne and Ludières). The studied outcrops are presented in detail below.

3. Detail sampling

Two outcrops were chosen for our ⁴⁰Ar/³⁹Ar investigation. They represent two different facies of the GN according to previous works (Pastre and Cantagrel, 2001; Vincent, 1979). One of the samples is located north of the proposed caldera limit (*i.e.* Rochefort-Montagne). The last one (*i.e.* Ludières) belongs to the numerous outcrops known north of Saint-Nectaire and belonging to the eastern extension of the GN (Fig. 1).

3.1. Rochefort-Montagne

We sampled in an old quarry northeast of the - Montagne town (entrance along D2089 road, 45°41′30″N; 2°48′30″E) (Fig. 2a). The GN outcrop is comprised 12–15-m-high white cliffs visible from the road (Fig. 2b). The facies found in this quarry consist of a white coherent rhyolite with only small (mainly <1 cm) and dispersed fibrous pumice stones. We collected the samples (*i.e.* 1 kg of homogeneous fine rhyolite with few pumice visible) on the cliff located east of the quarry, about 1 m above the current ground. Only centimetric darker rock xenoliths were visible to the naked eye. Because of the lack of large fibrous pumice stones and of the presence of surge deposits of similar composition

Fig. 2. Detailed maps of the two investigated GN outcrops with (a and b) Rochefort-Montagne quarry location and picture; (c and d) Ludières quarry location and photographs of the large white rhyolitic pumice stones found in this locality.

below the Rochefort-Montagne, this outcrop is interpreted as representing the early phase of the GN (Pastre and Cantagrel, 2001).

3.2. Ludières

The GN outcrops in two small quarries located 300 m northeast of the hamlet of Ludières (town of Vernet-Sainte-Marguerite) (45°37′12″N; 2°57′38″E), 12 km outside of the proposed caldera limits (Fig. 1). A minimum thickness of 8 m could be estimated for the GN in these quarries. The facies of the GN is distinct from the previous sample and consists mainly of large fibrous pumice stones (*i.e.* 4–6 cm, Fig. 2d) within a white coherent cindy matrix. This facies is interpreted as "the main eruptive phase" of the GN (Pastre, 1987). A similar facies is recognized in the nearby outcrop of Les Arnats (Fig. 1). We collected about 30 large fibrous pumice stones in several zones for our

investigation. Sanidine as well as edenite crystals were visible to the naked eyes in several pumice stones.

4. ^{40}Ar/^{39}Ar method

Because of the lack of large sanidine in the fibrous pumice stones in Rochefort-Montagne samples, we decided to separate sanidine from the coherent rhyolitic matrix, whereas we worked exclusively on the large fibrous pumice stones from Ludières. After crushing and sieving, sanidines ranging from 400 to 500 μm in size were handpicked under a binocular microscope and then slightly leached for 5 min in 7% HF acid. For each sample, about thirty crystals were handpicked and separately loaded in aluminum disks and irradiated in three different irradiations of 90 min (IRR 37 for Rochefort-Montagne) and 120 min (IRR 68 for Ludières). Irradiations were made in the β1 tube of the OSIRIS reactor (French Atomic Energy

Commission, Saclay, France). After irradiation, samples were transferred into a copper sample holder and loaded individually into a differential vacuum Cleartran© window. Crystals were individually fused using a Synrad CO_2 laser at 10–15% of nominal power (*ca.* 25 W). Ar isotopes were analyzed using a VG5400 mass spectrometer equipped with a single-ion counter (Balzers SEV 217 SEN) following the procedure outlined in Nomade et al. (2010). Each Ar isotope measurement consisted of 20 cycles of peak switching of the argon isotopes. Neutron fluence (*J*) was monitored by co-irradiation of Alder Creek sanidines (Nomade et al., 2005). These standards were placed in the same pit as the samples during irradiation. The *J* value for each sample was calculated from analyses of two ACs-2 single crystal measurements with a nominal age of 1.193 Ma ($\pm$ 0.5%) and using the total decay constant of Steiger and Jäger (1977). Mass discrimination was assessed by analysis of air pipettes throughout the analytical period, and was calculated relative to a $^{40}Ar/^{36}Ar$ ratio of 298.56 (Lee et al., 2006). Several proposed calibrations of the $^{40}Ar/^{39}Ar$ chronometer are currently in use, yielding ages that vary by ~1% (Kuiper et al., 2008; Renne et al., 2011). This implied a difference in the calibrated age for our samples within the reported total uncertainty. As a consequence, we used the values of Nomade et al. (2005) and of Steiger and Jäger (1977) for all the ages reported hereafter. Procedural blanks were measured every two or three unknowns. For a typical 10-min static blank, the backgrounds were generally about 3.0–4.0×10^{-17} and 6.0–7.0×10^{-19} moles for ^{40}Ar and ^{36}Ar, respectively. The nucleogenic production ratios used to correct for reactor-produced Ar isotopes from K and Ca are reported in the supplementary dataset (S1 and S2).

Because of the lack of large sanidine in the fibrous pumice stones in Rochefort-Montagne samples, we decided to separate sanidine from the coherent rhyolitic matrix, whereas we worked exclusively on the large fibrous pumice stones from Ludières. After crushing and sieving, sanidines ranging from 400 to 500 μm in size were handpicked under a binocular microscope and then slightly leached for 5 min in 7% HF acid. For each sample, about thirty crystals were handpicked and separately loaded in aluminum disks and irradiated in three different irradiations of 90 min (IRR 37 for Rochefort-Montagne) and 120 min (IRR 68 for Ludières). Irradiations were made in the β1 tube of the OSIRIS reactor (French Atomic Energy Commission, Saclay, France). After irradiation, samples were transferred into a copper sample holder and loaded individually into a differential vacuum Cleartran© window. Crystals were individually fused using a Synrad CO_2 laser at 10–15% of nominal power (*ca.* 25 W). Ar isotopes were analyzed using a VG5400 mass spectrometer equipped with a single-ion counter (Balzers SEV 217 SEN) following the procedure outlined in Nomade et al. (2010). Each Ar isotope measurement consisted of 20 cycles of peak switching of the argon isotopes. Neutron fluence (*J*) was monitored by co-irradiation of Alder Creek sanidines (Nomade et al., 2005). These standards were placed in the same pit as the samples during irradiation. The *J* value for each sample was calculated from analyses of two ACs-2 single crystal measurements with a nominal age of 1.193 Ma ($\pm$ 0.5%) and using the total decay constant of

Steiger and Jäger (1977). Mass discrimination was assessed by analysis of air pipettes throughout the analytical period, and was calculated relative to a $^{40}Ar/^{36}Ar$ ratio of 298.56 (Lee et al., 2006). Several proposed calibrations of the $^{40}Ar/^{39}Ar$ chronometer are currently in use, yielding ages that vary by ~1% (Kuiper et al., 2008; Renne et al., 2011). This implied a difference in the calibrated age for our samples within the reported total uncertainty. As a consequence, we used the values of Nomade et al. (2005) and of Steiger and Jäger (1977) for all the ages reported hereafter. Procedural blanks were measured every two or three unknowns. For a typical 10-min static blank, the backgrounds were generally about 3.0–4.0×10^{-17} and 6.0–7.0×10^{-19} moles for ^{40}Ar and ^{36}Ar, respectively. The nucleogenic production ratios used to correct for reactor-produced Ar isotopes from K and Ca are reported in the supplementary dataset (S1 and S2).

5. $^{40}Ar/^{39}Ar$ results

Analytical details for each measured crystal are reported in the supplementary dataset (Tables S1 and S2). Results are presented as probability diagrams (Deino and Potts, 1990) and inverse isochrones in Fig. 3. Weighted mean ages and uncertainties are calculated using IsoPlot 3.0 (Ludwig, 2001) and given at 95% of probability, including the *J* flux uncertainty. We also added the total uncertainty, therefore including the decay constant between brackets for each sample. A homogeneous juvenile population is considered relevant when the weighted mean of these crystals has a probability fit $\geq$0.1. The weighted average ages are calculated including the *J* uncertainty throughout the text.

Analytical details for each measured crystal are reported in the supplementary dataset (Tables S1 and S2). Results are presented as probability diagrams (Deino and Potts, 1990) and inverse isochrones in Fig. 3. Weighted mean ages and uncertainties are calculated using IsoPlot 3.0 (Ludwig, 2001) and given at 95% of probability, including the *J* flux uncertainty. We also added the total uncertainty, therefore including the decay constant between brackets for each sample. A homogeneous juvenile population is considered relevant when the weighted mean of these crystals has a probability fit $\geq$0.1. The weighted average ages are calculated including the *J* uncertainty throughout the text.

5.1. Rochefort-Montagne

A total of 14 sanidines were dated for this sample. The probability diagram is multimodal with four modes (Fig. 3a). The youngest population (juvenile population) is comprised of only four crystals and gives a weighted mean age of 2.76 $\pm$ 0.03 Ma (0.07 Ma; MSWD = 0.7, P = 0.5), which suggests the presence of mainly xenocrysts (70% of the crystals). Because of the low spread (94.7–96.5% of $^{40}Ar^*$) and of the limited number of juvenile crystals, we were not able to calculate a valid inverse isochrone (Fig. 3b and Table S1).

A total of 14 sanidines were dated for this sample. The probability diagram is multimodal with four modes (Fig. 3a). The youngest population (juvenile population) is comprised of only four crystals and gives a weighted
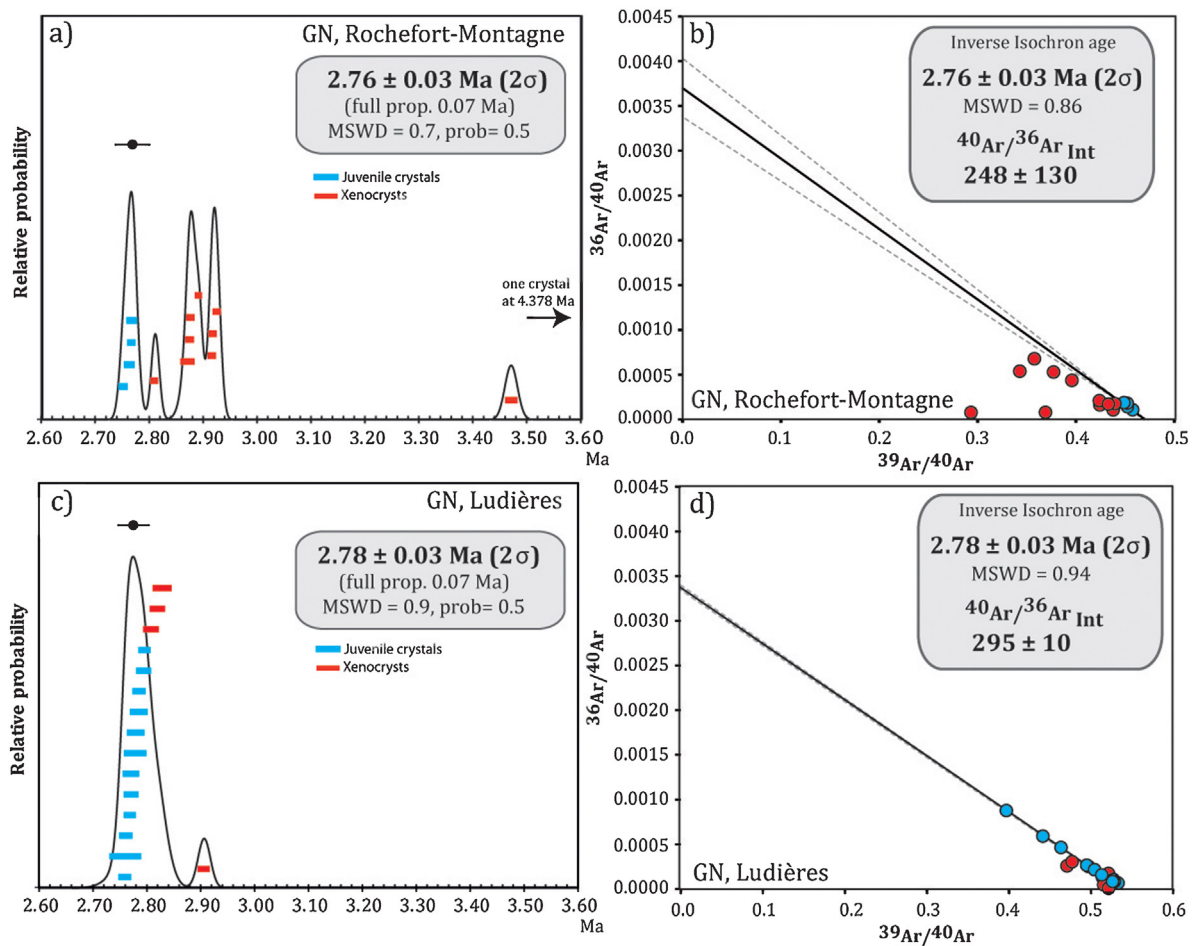
Fig. 3. ^{40}Ar/^{39}Ar results presented as probability diagrams and inverse isochrones.

mean age of 2.76 ± 0.03 Ma (0.07 Ma; MSWD = 0.7, P = 0.5), which suggests the presence of mainly xenocrysts (70% of the crystals). Because of the low spread (94.7–96.5% of ^{40}Ar*) and of the limited number of juvenile crystals, we were not able to calculate a valid inverse isochrone (Fig. 3b and Table S1).

5.2. Ludières

We measured a total of 16 crystals. Excluding one obviously older xenocryst and three crystals that created a small tail on the probability diagram, all other crystals (n = 12) belong to a juvenile population (Fig. 3c). These crystals allow calculating a weighted mean age of 2.78 ± 0.03 Ma (0.07 Ma; MSWD = 0.9, P = 0.5). The corresponding inverse isochrone age calculated using this juvenile population is self-coherent (i.e. 2.78 ± 0.03 Ma; MSWD = 0.9). The ^{40}Ar/^{36}Ar initial intercept (i.e. 295 ± 10) is equivalent to the atmospheric value (Fig. 3d and Table S2).

We measured a total of 16 crystals. Excluding one obviously older xenocryst and three crystals that created a small tail on the probability diagram, all other crystals (n = 12) belong to a juvenile population (Fig. 3c). These crystals allow calculating a weighted mean age of

2.78 ± 0.03 Ma (0.07 Ma; MSWD = 0.9, P = 0.5). The corresponding inverse isochrone age calculated using this juvenile population is self-coherent (i.e. 2.78 ± 0.03 Ma; MSWD = 0.9). The ^{40}Ar/^{36}Ar initial intercept (i.e. 295 ± 10) is equivalent to the atmospheric value (Fig. 3d and Table S2).

6. Discussion

The new ^{40}Ar/^{39}Ar age constraints we present bring a new and important contribution to the understanding of the GN and questioned hypotheses concerning its age and origin. First we will discuss the chronostratigraphic position of this event within the Guéry stratovolcano history of Nomade et al. (2014a). In a second phase, we will discuss the genetic link between this eruption and the cryptic "Haute Dordogne" caldera.

6.1. About the age of the GN

So far, the age of this major rhyolitic eruption relied on a multi-crystals ^{40}Ar/^{39}Ar investigation, made more than 25 years ago (Féraud et al., 1990). Since this work, the age of this eruption as well as that of the co-genetic caldera
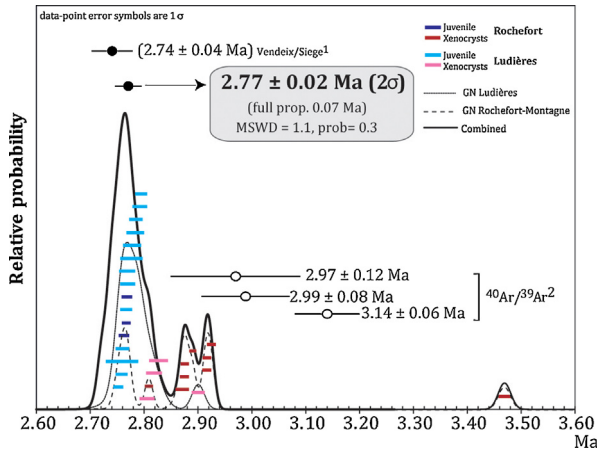
Fig. 4. Ludières and Rochefort-Montagne outcrops: combined $^{40}Ar/^{39}Ar$ probability diagram compared to the age of the "Vendeix-Siege" rhyolitic pumice stones (Nomade et al., 2014a). The $^{40}Ar/^{39}Ar$ multi-crystal ages of Féraud et al. (1990) are also reported in the figure. The blue boxes are for juvenile crystals, the red ones for xenocrysts.

presence of xenocrysts within the sanidine populations analyzed at the time (Fig. 4). We found more contamination in the Rochefort-Montagne sample (*i.e.* 70% of the crystals analyzed), probably because we worked on the crystals from the matrix rather than ones extracted from fibrous pumice stones. A xenocrystic contamination was also found in the "juvenile" Ludières large fibrous pumice stones that we investigated (Fig. 3). Such discrete xenocrystic populations are likely to have been incorporated into the magma very near or at the surface in a rapidly cooled pyroclastic flow; otherwise, it would have resulted in a total resetting of the K/Ar isotopic system (*e.g.*, Spell et al., 2001). Our results explain why previous attempts at accurately dating this event were unsuccessful. The ages we obtained for Rochefort-Montagne and Ludières are indeed identical within uncertainty limits with that of the rhyolitic "Vendeix-Siège" formation (*i.e.* 2.74 ± 0.02 Ma; Nomade et al., 2014a) (Fig. 4). Based on this new geochronological data as well as on geochemical and mineralogical similarities, this proves that these formations belong to the same event as the one first suggested by Pastre (1987). According to these new pieces of information, we could with confidence say that the position of the GN within the history of the Mont-Dore Massif should now be reconsidered.

Following the tephro-stratigraphic history proposed by Nomade et al. (2014a), the GN ignimbrite could now be incorporated into the G.II phase of the Guéry and cannot be considered anymore as part of the early activity of this stratovolcano (G.I of Nomade et al., 2014a) (Fig. 5). We now proposed that the Guéry stratovolcano explosive history started with rather small rhyolitic eruptions scattered between 3.10 and 3.00 Ma (G.I phase, Fig. 5). This early
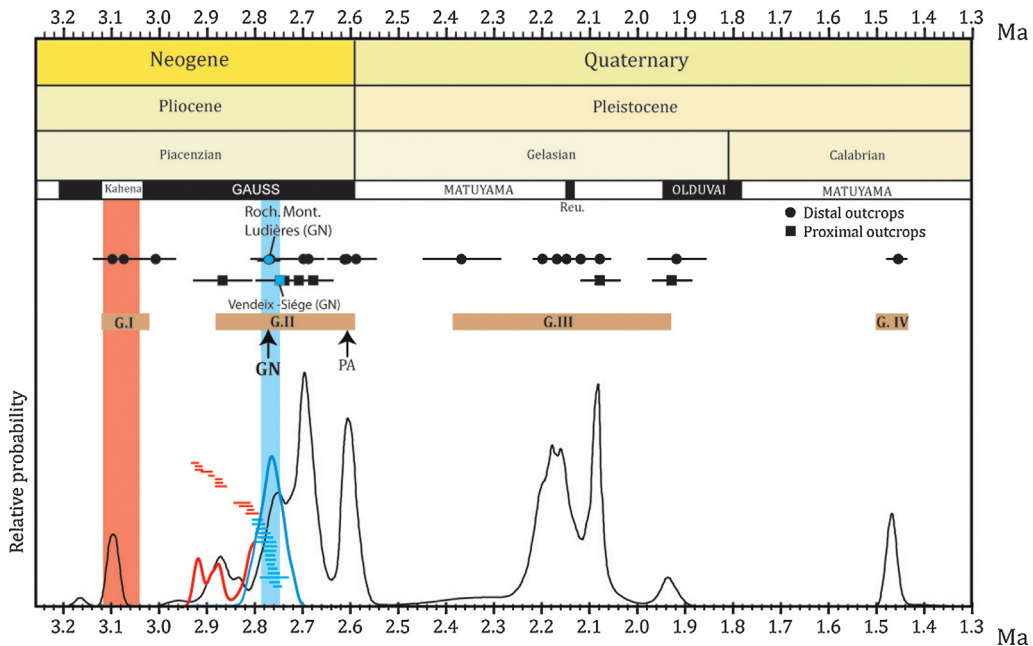
was fixed at 3.07 ± 0.04 Ma, early in the history of the Mont-Dore Massif (Nomade et al., 2014a; Pastre and Cantagrel, 2001). The ages of 2.78 ± 0.03 Ma and 2.76 ± 0.03 Ma that we obtained for the Rochefort-Montagne and Ludières outcrops, respectively, are 300 ka younger than expected. We combined in Fig. 4 both results and obtained a weighted age of 2.77 ± 0.02 Ma (0.07 Ma, $n = 16$, MSWD = 1.1; $P = 0.3$). We considered this age to be the more accurate one for the GN eruption. The difference in age between our work and the age obtained by Féraud et al. (1990) is easily explained by the

Fig. 5. Chronology of the pyroclastic units of the Guéry stratovolcano modified from Nomade et al. (2014a). The new $^{40}Ar/^{39}Ar$ single-crystal analyses (blue for juvenile crystals, red for xenocrysts) and the corresponding probability diagram are superposed on the previous results of Nomade et al. (2014a,b). GN and PA correspond to the Grande Nappe and the Perrier debris avalanches (flank collapses of the Guéry), respectively. The PA marks the end of the main explosive activity of cycle "G. II" of the Guéry stratovolcano as defined by Nomade et al. (2014a). The blue strip corresponds to the new age for the GN, whereas the red one corresponds to the previously suggested age (Féraud et al., 1990).

phase is now found at the base of the Perrier sequence (Nomade et al., 2014b; Pastre, 2004). This initial explosive phase was followed by a trachytic explosive activity at the beginning of the G.II phase (Fig. 5). This activity is well preserved in the Vendeix area, such as in the so-called "Bourboule bas" pyroclastic unit we previously dated back to 2.86 ± 0.02 Ma (see fig. 9 in Nomade et al., 2014a). The GN eruption has occurred 2.77 ± 0.02 Ma ago, in the middle of the G.II phase (GN in Fig. 5). In this new tephrostratigraphic history, the GN preceded by only 200 ka (*ca.* 2.60–2.58 Ma) the four lateral flank collapses that affected the Guéry stratovolcano (Bernard et al., 2009; Nomade et al., 2014a; PA in Fig. 5). The new tephrostratigraphic history summaries above involved that most of the pyroclastic products of the Guéry were emplaced in a relatively short period of time (*i.e.* 2.86–2.58 Ma) during the G.II phase. This has to be linked with high magma production rates during this phase of the Guéry stratovolcano as well as with particular conditions in the magmatic chamber(s) that would require further investigations. The comparison between the new single-crystal analyses from the GN outcrops and the previously published ages suggest that a majority of the contamination found within the GN belongs to the trachytic episode occurring at the beginning of the G.II phase (Fig. 5).

6.2. About the link with the cryptic "Haute-Dordogne" caldera

As said above, Nomade et al. (2014b) also dated a rhyolitic pumiceous fall below what is considered to be the GN in the Perrier plateau, which is much older than the GN. As a consequence, the proposed volume of 5–6 km^3 should be taken with great caution, as some rhyolitic outcrops are not linked to the GN eruption. However, as we do not systematically investigate all rhyolitic outcrops, it will remain hazardous to propose a more precise volume without a more widespread study. The existence of two calderas (C.I for the Guéry and C.II for the Sancy) within the Mont-Dore Massif was heavily debated, especially because their existence is mainly based on geophysical investigation, therefore only on indirect evidences (*e.g.*, Cantagrel and Briot, 1990; Lavina, 1985; Ménard et al., 1980; Mossand, 1983; Nercessian et al., 1984; Varet et al., 1980; Vincent, 1980). The location and size of the C.I "Haute Dordogne" caldera is still an open question: centered on the La Bourboule area for some authors (Ménard et al., 1980; Varet et al., 1980; Vincent, 1980; Fig. 1), it was also proposed to be closer to the Guéry Lake area where some differentiated domes may mark the edge of the caldera (Cantagrel and Briot, 1990). This last hypothesis could be rejected as we know that some domes are much younger than the GN (*e.g.*, 2.095 ± 0.038 Ma (U–Pb age) for Sanadoire; Cocherie et al., 2009) related to cycle G.III of the Guéry area (Nomade et al., 2014a; Fig. 5). Some other domes were emplaced following several eastern flank collapses of the Guéry stratovolcanoes that mark the end of cycle G.II (Perrier Avalanche; PA in Fig. 5), and therefore there is probably no link with a caldera formation occurring 200–300 ka before. One of the arguments put forward to prove the existence of the Haute–Dordogne caldera is the widespread ignimbrite GN supposed

to be emplaced early in the Guéry stratovolcano history. The position of the GN within the volcano-sedimentary infilling of the supposed caldera does not support a genetic link between the depression and/or low speed anomalies (*i.e.* Nercessian et al., 1984; Varet et al., 1980) observed around the La Bourboule area and the GN eruption itself. The circular structure within the basement highlighted by Nercessian et al. (1984) argues in favor of the existence of a depression interpreted as a "caldera" by the authors. We would like here to notice that the age of such a structure is unknown and cannot be directly linked to the GN at 2.77 Ma. Furthermore, this circular depression is based on extremely low-resolution 3D seismic data compared to the current state of the art of technology. Another observation which could be made is that the caldera limits suggested by this circular structure include the so-called C.2 caldera (Lavina, 1985), which is much younger, dated back to 719 ± 20 ka (full external uncertainty; Nomade et al., 2012). This depression also includes geographically the younger (250-m-thick) pyroclastic rocks pile outcropping in the Mont-Dore Valley dated back to between 640 and 390 ka (Nomade et al., 2012). This suggests that the low-speed zone highlighted by Nercessian et al. (1984) is mainly found below unconsolidated pyroclastic materials of various ages, covering 3.0 Ma of volcanic history, two superposed stratovolcanoes, and eight pyroclastic cycles (Nomade et al., 2014a). In conclusion, it is impossible to link this circular structure to any specific eruption cycle or period of activity of the Mont-Dore Massif. Finally, according to the proposed volumes and various sizes of the caldera, the GN would have left a depression of about 200–250 m in depth (Cantagrel and Briot, 1990), which is not compatible with the geophysical and geological evidences put forward by Ménard et al. (1980), Nercessian et al. (1984), Varet et al. (1980), and Vincent (1980), who all suggested a much larger and deeper caldera. It remains that we cannot reject the hypothesis that the GN is link to a caldera formation but this hypothesis currently lacks geological, geophysical, and geochronological evidence. If the circular structure within the basement known as "Haute Dordogne" caldera really exists, has this structure been likely formed before the GN eruption? This is a hypothesis that needs to be considered; however, the question is: where are the co-eruptive deposits resulting from its formation? One thing is certain: it is neither the small-volume rhyolitic eruption found reworked at the base of the Perrier plateau, nor the tuffites and trachytic flows below the GN around La Bourboule, which could be linked to the formation of a large caldera.

To finalize this discussion, we would like here to explore another hypothesis: has the GN been generated by a northward-trending lateral blast, or is it rather linked to the formation of a caldera? With such mechanism, the co-eruptive products are deposited northward first, following the blast, and then along an east–west direction channeled by the Paleo-Allier valley system. This hypothesis explained the position of the GN within the Vendeix–La Bourboule volcano-sedimentary succession as well as the current outcrops of the GN found along the northern and southern edges of the Vernet stream (Fig. 1). The same channeling processes have occurred after the four collapses of the eastward part of the Guéry stratovolcano dated back to between 2.60 and 2.58 Ma (Nomade et al., 2014a)

(PA in Fig. 5). We currently cannot favor any hypothesis, but our work clearly shows that many things are still unresolved and that works mainly done more than 30 years ago need to be reevaluated in the light of the state of the art of analytical techniques. Despite the recent investigations that improved our knowledge of the Mont-Dore Massif, more geochronology, geochemistry and geophysics studies are critically needed in the future to decipher the origin of the GN, but also reconstruct the eruptive history and geochemical evolution of the second largest differentiated volcanic massif of Europe.

7. Conclusions

The new single crystals ^{40}Ar/^{39}Ar investigation led us to the following conclusions:

(1) the GN eruption is now precisely dated back to 2.77 ± 0.02 Ma (0.07 Ma full external uncertainty) and belongs to the G.II phase of the Guéry stratovolcano;
(2) the previously proposed ^{40}Ar/^{39}Ar age was corrupted by unrecognized xenocrystic contamination;
(3) the correlation made between the Vendeix rhyolitic complexes (intra-caldera position) dated back to 2.74 ± 0.04 Ma and the GN is now firmly established;
(4) we propose an alternate hypothesis for the formation of the GN: a northward blast eruption channeled later eastward toward the paleo-Allier River.

Acknowledgments

Appendix A. Supplementary data

Supplementary data associated with this article can be found, in the online version, at http://dx.doi.org/10.1016/j.crte.2017.02.003.

References

Bernard, B., Van Wyk de Vries, B.μ., Leyrit, H., 2009. Distinguishing volcanic debris avalanche deposits from their reworked products: the Perrier sequence (French Massif Central). Bull. Volcanol. 71, 1056–1071.

Besson, J.-C., 1978. Les formations volcaniques du versant oriental du massif du Mont-Dore (Massif central français), feuille 1/25 000e Veyre-Monton 5-6. Thèse 3e cycle, Clermont-Ferrand, France.

Brousse, R., 1963. Identification de deux coulées de ponces dans le massif volcanique du Mont-Dore (Auvergne). C. R. Acad. Sci. Paris, Ser. D 257, 2869–2871.

Brousse, R., 1971. Magmatologie du volcanisme néogène et quaternaire du Massif central. In: Symposium Géologie, géomorphologie et structure profonde du Massif central français, Plein Air Service, Clermont-Ferrand, pp. 377–478.

Brousse, R., 1984. Comblement de la fosse volcanique et socle du massif du Mont-Dore in Programme géologie profonde de la France. Thème 9, Volcanisme récent du Massif central (Mont-Dore). Doc. BRGM 81–9, 9–19.

Brousse, R., Lefèvre, C., 1966. Nappes de ponces du Cantal et du Mont-Dore. Leurs aspects volcanologiques, pétrographiques et minéralogiques. Bull. Soc. geol. France 7, 223–245.

Cantagrel, J.-M., Baubron, J.-C., 1983. Chronologie K-Ar des éruptions dans le massif volcanique des Monts-Dore: implications volcanologiques. Geol. France 2, 123–142.

Cantagrel, J.-M., Briot, D., 1990. Avalanches et coulées de débris: le Volcan du Guéry – Où est la caldera d'effondrement dans le massif des Monts Dore? C. R. Acad. Sci. Paris, Ser. D 311, 219–225.

Cocherie, A., Fanning, C.M., Jezequel, P., Robert, M., 2009. LA-MC-ICPMS and SHRIMP U–Pb dating of complex zircons from Quaternary tephras from the French Massif Central: magma residence time and geochemical implications. Geochim. Cosmochim. Acta 73, 1095–1108.

Cas, R.A.F., Wright, J.V., 1988. Volcanic Successions. Modern and Ancient. Unwin Hyman, 528 p.

Degeai, J.-P., Pastre, J.-F., Gauthier, A., Robert, V., Nomade, S., Bout-Roumazeilles, Guillou, H., 2013. La séquence lacustre du maar d'Alleret (Massif central, France): Téphrochronologie et évolution paléoenvironnementale en Europe occidentale au début du Pléistocène moyen. Quaternaire 24, 443–449.

Deino, A., Potts, R., 1990. Single-crystal ^{40}Ar/^{39}Ar dating of the Olorgesailie Formation, Southern Kenya Rift. J. Geophys. Res. 95, 8453–8470.

Féraud, G., Lo Bello, P., Hall, C.M., Cantagrel, J.M., York, D., Bernat, M., 1990. Direct dating of Plio-Quaternary pumices by ^{40}Ar/^{39}Ar step-heating and single-grain laser fusion methods: the example of the Monts-Dore massif (Massif Central, France). J. Volcanol. Geotherm. Res. 40, 39–53.

Kuiper, K.F., Deino, A., Hilgen, F.J., Krijgsman, W., Renne, P.R., Wijbrans, J.R., 2008. Synchronizing rock clocks of Earth history. Science 320, 500–504.

Lavina, P., 1985. Le volcan du Sancy et le « Massif adventif ». Études volcanologiques et structurales. (Ph.D. thesis). Université de Clermont-Ferrand, France, 211 p.

Lee, J.Y., Marti, K., Severinghaus, J.P., Kawamura, K., Yoo, H.-S., Lee, J.B., Kim, J.S., 2006. A redetermination of the isotopic abundances of atmospheric Ar. Geochim. Cosmochim. Acta 70, 4507–4512.

Ludwig, K.R., 2001. Isoplot 3.0a geochronological toolkit for Microsoft Excel. In: Special Publication No. 4. Berkeley Geochronology Center, Berkeley, CA, USA.

Ly, M.H., 1982. Le Plateau de Perrier et la Limagne du Sud: Études volcanologiques et chronologiques des produits montdoriens (Massif central français). Thèse de 3e cycle. , Clermont-Ferrand, France, 180 p.

Ménard, J.-J., 1979. Contribution à l'étude pétrographique des nappes de ponces du massif volcanique du Mont-Dore (Massif central français). Thèse de 3e cycle. Université Paris-Sud, Orsay, 105 p.

Ménard, J.-J., Clocchiatti, R., Maury, R.C., Brousse, R., 1980. Origine des ponces rhyolitiques du Mont-Dore (Massif central, France): Arguments pétrologiques. C. R. Acad. Sci. Paris, Ser. D 290, 559–562.

Mossand, P., 1983. Le volcanisme anté-et syn-caldera des Monts-Dore (Massif central français). Implications géothermiques. (Ph.D. thesis). Université de Clermont-Ferrand, France, 197 p.

Mossand, P., Cantagrel, J.-M., Vincent, P., 1982. La caldera de Haute Dordogne: âge et limites (massif des Monts-Dore, France). Bull. Soc. geol. France 7, 727–738.

Nercessian, A., Hirn, A., Tarantola, A., 1984. Three-dimensional seismic transmission prospecting of the Mont-Dore volcano, France. Geophys. J. R. Astron. Soc. 76, 307–315.

Newhall, C.G., Self, S., 1982. The volcanic explosivity index (VEI): an estimate of explosive magnitude for historical volcanism. J. Geophys. Res. 87, 1231–1238.

Nomade, S., Renne, P.R., Vogel, N., Deino, A.L., Sharp, W.D., Becker, T.A., Jaouni, A.R., Mundil, R., 2005. Alder Creek sanidine (ACs-2): a Quaternary ^{40}Ar/^{39}Ar dating standard tied to the Cobb Mountain geomagnetic event. Chem. Geol. 218, 315–338.

Nomade, S., Gauthier, A., Guillou, H., Pastre, J.-F., 2010. ^{40}Ar/^{39}Ar temporal framework for the Alleret maar lacustrine sequence (French Massif Central): volcanological and paleoclimatic implications. Quat. Geochem. 5, 20–27.

Nomade, S., Scaillet, S., Pastre, J.-F., Nehlig, P., 2012. Pyroclastic chronology of the Sancy stratovolcano (Mont-Dore, French Massif Central): new high-precision ^{40}Ar/^{39}Ar constraints. J. Volcanol. Geotherm. Res. 225–226, 1–12.

Nomade, S., Pastre, J.-F., Nehlig, P., Guillou, H., Scao, V., Scaillet, S., 2014a. Tephrochronology of the Mont-Dore volcanic Massif (Massif Central, France). New ^{40}Ar/^{39}Ar constraints on the Late Pliocene and Early Pleistocene activity. Bull. Volcanol. 76, 798.

Nomade, S., Pastre, J.-F., Guillou, H., Faure, M., Guérin, G., Delson, E., Debard, E., Voinchet, P., Messager, E., 2014b. ^{40}Ar/^{39}Ar constraints on some French landmark Late Pliocene to Early Pleistocene large

mammalian paleofauna: paleoenvironmental and paleoecological implications. Quat. Geochronol. 21, 2–15.

Pastre, J.-F., 1987. Les formations plio-quaternaires du bassin de l'Allier et le volcanisme régional (Massif central, France). Thèse. Université Pierre-et-Marie-Curie (Paris VI). Mém. Sci. Terre 87-32, 733 p.

Pastre, J.-F., 2004. The Perrier Plateau: a Plio-pleistocene long fluvial record in the river Allier Basin, Massif Central, France. Quaternaire 15, 87–102.

Pastre, J.-F., Cantagrel, J.-M., 2001. Téphrostratigraphie du Mont-Dore (Massif central, France). Quaternaire 12 (4), 249–267.

Pastre, J.-F., Debard, E., Nomade, S., Guillou, H., Faure, M., Guérin, C., Delson, E., 2015. Nouvelles données géologiques et téphrochronologiques sur le gisement paléontologique du maar de Senèze (Pléistocène inférieur, Massif central, France). Quaternaire 26 (3), 225–244.

Renne, P.R., Balco, G., Ludwig, K., Mundil, R., Min, K., 2011. Response to the Comment by W. H. Schwarz et al., on "Joint determination of ^{40}K decay constants and ^{40}Ar/^{40}K for the Fish Canyon sanidine standard, and improved accuracy for ^{40}Ar/^{39}Ar geochronology" Geochim. Cosmochim. Acta 75, 5097–5100.

Spell, T.L., Smith, E.I., Sanford, A., Zanetti, K.A., 2001. Systematics of xenocrystic contamination: preservation of discrete feldspar populations at McCullough Pass Caldera revealed by ^{40}Ar/^{39}Ar dating. Earth Planet. Sci. Lett. 190, 153–165.

Steiger, R.H., Jäger, E., 1977. Subcommission on geochronology: convention on the use of dacay constants in geo- and cosmochronology. Earth Planet. Sci. Lett. 36, 359–362.

Varet, J., Stieltjes, L., Gerard, A., Fouillac, C., 1980. Prospection géothermique intégrée dans le massif du Mont-Dore. In: Advances in European Geothermal Research. Reitel Publishing, Strasbourg, France155–201.

Villemant, B., Joron, J.-L, Treuil, M., 1980. Origine des quartz des nappes de ponces du Mont-Dore (Massif central, France): arguments géochimiques. C. R. Acad. Sci. Paris, Ser. D 290, 687–690.

Vincent, P.M., 1979. Un repère chronologique dans la caldéra des Monts Dore (Massif central français): les pyroclastites du dôme de la Gacherie. C. R. Acad. Sci. Paris, Ser. D 289, 1009–1012.

Vincent, P.M., 1980. Volcanisme et chambres magmatiques: l'exemple des Mont-Dore. Livre jubilaire de la Société géologique de France. Mém. hors-série 10, 71–85.